A method for characterizing adsorption of flowing solutes to microfluidic device surfaces†

Kenneth R. Hawkins,*[a] Mark R. Steedman,*[b] Richard R. Baldwin,[a] Elain Fu,[a] Sandip Ghosal[c] and Paul Yager[a]

Received 6th September 2006, Accepted 23rd November 2006
First published as an Advance Article on the web 18th December 2006
DOI: 10.1039/b612894g

We present a method for characterizing the adsorption of solutes in microfluidic devices that is sensitive to both long-lived and transient adsorption and can be applied to a variety of realistic device materials, designs, fabrication methods, and operational parameters. We have characterized the adsorption of two highly adsorbing molecules (FITC-labeled bovine serum albumin (BSA) and rhodamine B) and compared these results to two low adsorbing species of similar molecular weights (FITC-labeled dextran and fluorescein). We have also validated our method by demonstrating that two well-known non-fouling strategies [deposition of the polyethylene oxide (PEO)-like surface coating created by radio-frequency glow discharge plasma deposition (RF-GDPD) of tetraethylene glycol dimethyl ether (tetraglyme, $CH_3O(CH_2CH_2O)_4CH_3$), and blocking with unlabeled BSA] eliminate the characteristic BSA adsorption behavior observed otherwise.

Introduction

The non-specific adsorption of proteins to surfaces is a complex phenomenon[1] that is of particular concern in the high surface-to-volume-ratio environments of microfluidic channels.[2] In fluorescence-based assays, labeled analytes adsorbed to channel walls increase the background signal, complicating analysis.[3] Non-specific adsorption upstream of detection can also lead to an unpredictable reduction in the concentration of an assay component.[4] Non-permanent or transient adsorption can slow the transport of analytes in microfluidic devices and can be particularly problematic when the timing of delivery of analyte or reagent is important.[5]

Much of data on nonspecific adsorbtion has been gathered under conditions that do not monitor both long-lived and transient adsorption.[1] One common method for monitoring adsorption has been to examine residual material left on the device after a typical use.[6,7] Although this is a direct and rather simple method that offers the advantage of *in situ* observation, it completely ignores transient adsorption. A more useful approach would allow for the monitoring of both long-lived and transient adsorption in a device that has similar dimensions, materials, flow parameters, *etc.* as the actual chip design under consideration.

We present a method for characterizing transient and long-lived adsorption of molecules of interest under flow in a representative microfluidic device. The device investigated here is simple, but the technque should extend to arbitrary channel geometries. Additionally, this method can be used to test anti-fouling surface modifications.[7–16] Successful anti-fouling surface modifications would eliminate the need for more complex fluidics (such as sheath flow[4]) to avoid surface adsorption problems.

Experimental

Device design and fabrication

The device design (Fig. 1) consisted of a main channel with large surface area for analyte adsorption and strategically placed inlet and outlet for simultaneous optical interrogation. The main channel was cut from a sheet of 0.10 mm thick pressure sensitive adhesive coated Mylar™ D (Fralock, Santa Clara, CA, USA) using a 25 W CO_2 laser (Universal Laser Systems, Scottsdale, AZ, USA). The top and bottom capping layers were cut from the same Mylar™ with no adhesive. Devices were pressed in an Atlas E–Z Press (International Crystal Laboratories, Garfield, NJ, USA) at 20.7 MPa for 20 min at room temperature to ensure an adequate seal.

Fluid delivery system

An Upchurch M-435 micro-injection valve (Upchurch Scientific, Oak Harbor, WA, USA) was used to introduce a pulse of analyte ($\sim$940 nL) to the device ($\sim$9.8 μL) mounted into a custom-built manifold. A positive displacement syringe (50 μL) pump (Kloehn, Las Vegas, NV, USA) was used to drive flow at a rate of 42 nL s^{-1}.

[a]*Department of Bioengineering, University of Washington, Seattle, WA, USA. E-mail: khawk@u.washington.edu; Fax: 1 206.543.3928; Tel: 1 206.543.9374*
[b]*UCSF/UC Berkeley Joint Graduate Group in Bioengineering, University of California at San Francisco and Berkeley, San Francisco, CA, USA. E-mail: mark.steedman@ucsf.edu.; Fax: 1 415.476.2414; Tel: 1 415.514.9695*
[c]*Department of Mechanical Engineering, Northwestern University, Evanston, IL, USA. Fax: 1 847.491.3915; Tel: 1 847.467.5990*
† Electronic supplementary information (ESI) available: Higher concentration FITC-BSA, nonfouling BSA coating, and simple predictive modeling. See DOI: 10.1039/b612894g

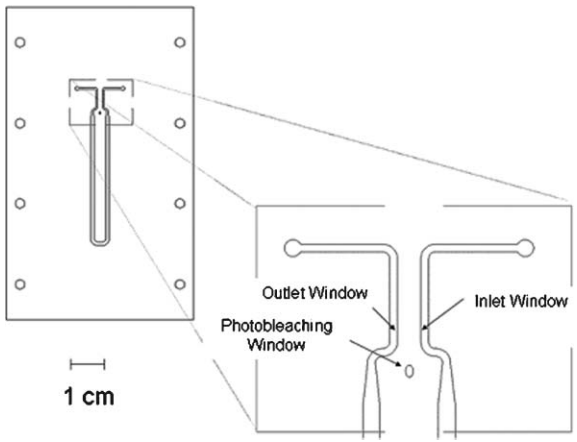

Fig. 1 The microfluidic channel used as an adsorption chromatography device. The channel shown above is cut into 0.10 mm thick Mylar coated with adhesive on both sides, and laminated with two 0.10 mm thick Mylar capping layers, one of which is cut with port holes to enable fluidic connections. The holes on the right and left margins are for mounting into a stage adapter and manifold. The main channel is 1 mm wide, and over 70 mm long, so that the device presents 204 mm^2 of surface to the 0.94 mm^3 (940 nL) of sample pulse, a surface to volume ratio of 217 mm^{-1}. Thus, by using dilute solutions of protein, and slow flow rates to allow sufficient time for protein diffusion, it is expected that a significant fraction of the protein in solution will be able to sample the surface, resulting in a detectable change between the incoming and eluted peaks (beyond expected dispersion) when adsorption is an important phenomena.

Instrumentation

A Zeiss ICM-405 inverted, epifluorescence microscope (Carl Zeiss Inc., Thornwood, NY, USA) was used to image each device over a 3.43 mm × 2.74 mm region. The excitation light source was a Zeiss HB100W mercury arc lamp (Carl Zeiss Inc., Thornwood, NY, USA) conditioned using a fluorescein filter set and a rhodamine filter set (Chroma Technology, Battleboro, VT, SA). A Retiga 1300 cooled, 12 bit CCD camera (QImaging, Burnaby, BC, Canada) was used for detection (exposure times of 1 and 2 s). Automated data acquisition was performed using a custom-coded LabVIEW (National Instruments, Austin, TX, USA) program and the image analysis was completed using a custom-coded MATLAB program (The MathWorks Inc., Novi, MI, USA).

Device pre-conditioning

A new device was used for each experiment. Prior to use, a device was photobleached by exposure to light from a UV transilluminator (Ultra Lum Inc., Paramount, CA, USA) for 1 h and the microscope light source for 20 min. It had been determined that untreated Mylar™ has significant autofluorescence which photobleaches with complex kinetics.[17] However, we determined that the photobleaching of our preconditioned Mylar™ devices can be fitted with a straight line, enabling simple data normalization.

Reagents

Solutions of varying concentrations of fluorescein (Sigma Chemicals, St. Louis, MO, USA), FITC-labeled dextran (MW 70 000, Sigma Chemicals, St. Louis, MO, USA), FITC-labeled BSA (Sigma Chemicals, St. Louis, MO, USA), and unlabeled BSA were prepared in 100 mM HEPES buffer, pH 7.5 (Sigma Chemicals, St. Louis, MO, USA). Rhodamine B (Sigma Chemicals, St. Louis, MO, USA) prepared in PBS buffer, pH 7.4 (Sigma Chemicals, St. Louis, MO, USA) was also used. The fluorescein (390 D) and FITC-dextran (70 kD) were assumed to be low-adsorbing; *i.e.*, function as negative controls. The rhodamine B (450 D) and FITC-BSA (68 kD) were expected to adsorb strongly, *i.e.*, function as positive controls.

Procedure

Each experiment consisted of five sequential injections of sample solution. First, the device was primed with an excess of buffer (~5 mL). In between sample injections, 100 μL of buffer was pushed through the device to purge any sample that had not strongly adsorbed to the device walls. Images were captured once every 10 s, beginning when the pump was started, until the intensity observed at the outlet reached a steady state. After five sample injections, the channel was flooded with sample solution and an image captured to enable flat-field correction of the data.

The intensity of fluorescence was sampled at each time point in three 10 pixel by 10 pixel (26.8 μm × 26.8 μm) detection windows defined within the inlet and outlet legs of the channel, and within a 'photobleaching window.' The raw data was then processed to obtain a corrected signal at each time point, $I_{corri} = I_{rawi} - (mt_i + B_0)$. Here I_{rawi} is the uncorrected intensity at time point specified by index i, t_i is the time point at index i, m is the slope of the photobleaching trendline from Excel (Microsoft, Redmond, WA, USA), and B_0 is the initial background intensity. A uniform rate of photobleaching in the three detection windows was assumed (the device location was adjusted with each experiment to ensure the photon flux was approximately uniform across the three locations). The inlet and outlet signals were flat-field corrected through division by the corresponding flood image values and normalized to the area under the inlet curve. The ratio of areas reflects the fraction of input mass that arrived at the outlet of the device.

Several experiments involving devices pretreated with nonfouling coatings were performed. Devices were exposed to tetraglyme RF-GDPD to produce a PEO-like coating using a method previously described,[10,11] or treated with unlabeled 20 μM BSA solution for 5 min (no flow) and then rinsed with buffer. Both were tested with BSA as the sample analyte.

Results and discussion

Experimental results with the adsorption characterization system show that it is capable of detecting both transient and long-lived adsorption in microfluidic devices.

Results with fluorescein (Fig. 2a) illuminate the performance of the system in the absence of significant adsorption. The high degree of peak superposition in the five within-experiment-runs indicates that this system can be operated with high precision. The return to baseline indicates that no long-lived adsorption to the detection window has occurred. The progress

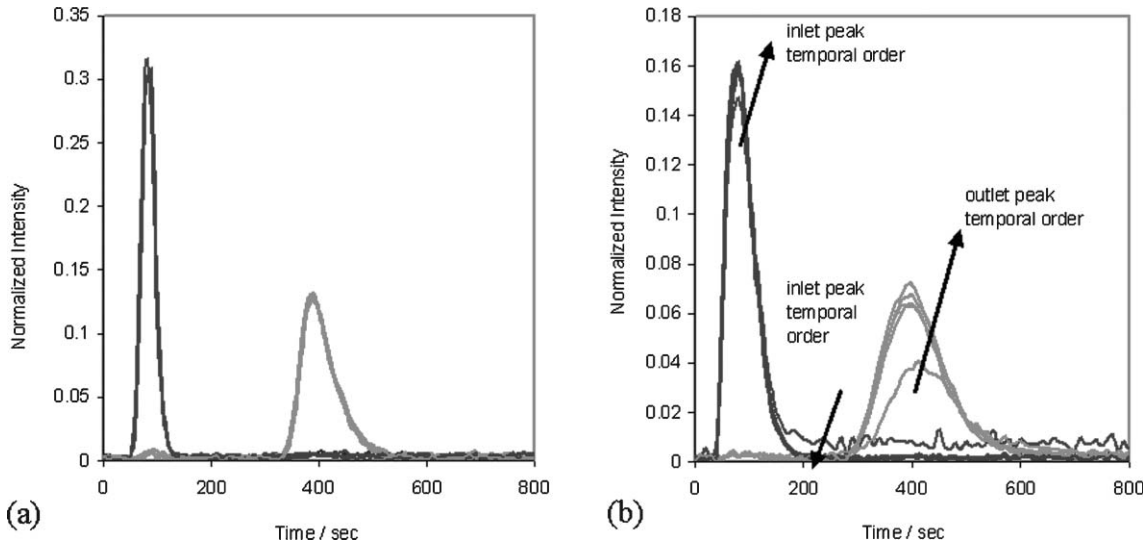

Fig. 2 Five representative runs for low-adsorbing negative controls. Dark grey lines are observations at the inlet, and light grey lines are observations at the outlet, with the data processing described in the text. A smooth interpolation is used for display. (a) Fluorescein shows little variation in the five runs with completely resolved inlet and outlet peaks. (b) FITC-dextran shows slight differences in the inlet and outlet peaks correlated with the temporal run order.

of the centroid of the peak is an estimate of the retention time of the mobile phase, which can be used to indicate if the elution of a test species has been slowed by transient adsorption.

The amount of dispersion in the peaks is greater for the higher molecular weight FITC-dextran relative to the lower molecular weight fluorescein. The results for FITC-dextran (Fig. 2b) suggest that it is not actually a negative control. The pattern of run-dependent changes in inlet baseline and eluted peak area look very similar to what was observed for higher concentrations of FITC-BSA (ESI†).

Both positive controls, rhodamine B (Fig. 3a) and FITC-BSA (Fig. 3b) clearly show the presence of adsorption, as evidenced by the differences in the chromatograms compared to negative controls of the same approximate diffusivity. The location of the centroid of the outlet peak of rhodamine B is clearly later than that of fluorescein, and the peaks are very tailed—observations that strongly suggest transient adsorption. The eventual return of the inlet chromatograms to baseline, however, indicate that no long-lived adsorption has occurred and is consistent with the models for small molecule adsorption. We hypothesize that the artifact at the early time points (*i.e.* lack of a flat baseline except for the first run) before the inlet peak has entered the inlet window is caused by rhodamine adsorbtion to upstream tubing and that the rinsing between

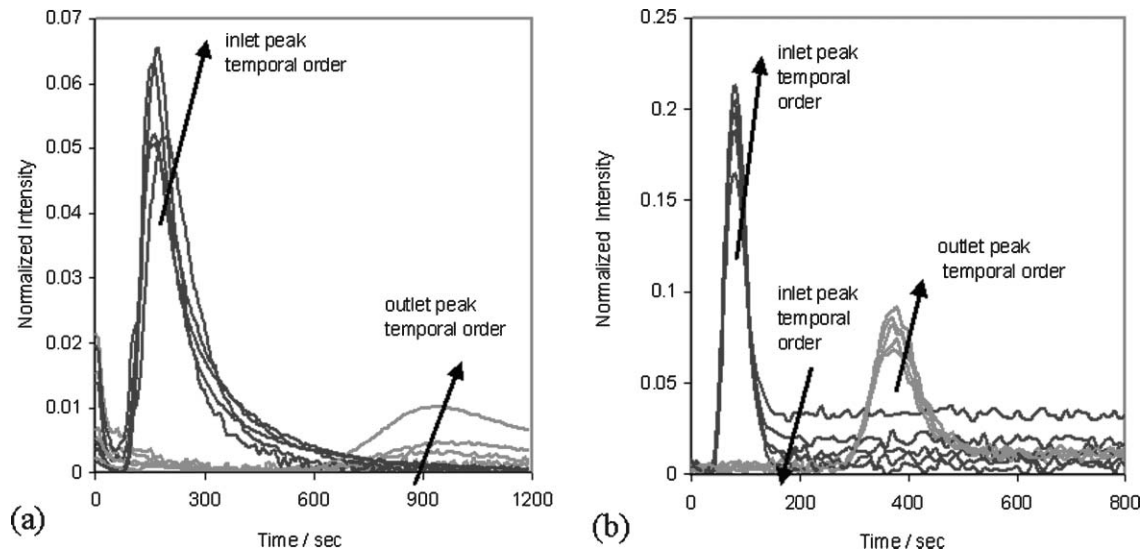

Fig. 3 Five representative runs for strongly adsorbing positive controls. Dark grey lines are observations at the inlet, and light grey lines are observations at the outlet, with the data processing described in the text. A smooth interpolation is used for display. (a) Rhodamine displays a much greater amount of dispersion than expected for a molecule of its size. (b) FITC-BSA (2 M) displays inlet and outlet peaks that do not return to baseline, a trend that is strongest at the initial inlet peak.

experiments did not completely remove residual rhodamine from the tubes.

In the FITC-BSA results, the elevation of the chromatogram baselines to a new steady state after the passing of the sample pulse, suggest that long-lived adsorption is occurring on the time scale of the experiment. The increased variance of the peak and the asymmetric tail suggest a transient adsorption component as well. The location of the centroid does not appear to be greatly affected, indicating that most of the adsorbing FITC-BSA attaches with a low dissociation rate: an observation that is consistent with what is known about BSA adsorption. We hypothesize that the peak seen at the outlet is comprised of the FITC-BSA mass that never adsorbed to the surface at all. The RMS distance that a molecule can be expected to diffuse in a given time period can be estimated using the relationship $\langle x \rangle = \sqrt{2Dt}$. Calculation, assuming a residence time in the channel of $\sim$300 s and a diffusivity for a BSA molecule of $D \approx 6 \times 10^{-7}$ cm^2 s^{-1}, results in $\langle x \rangle \cong 190$ μm. This implies that most BSA molecules should sample the top and bottom surfaces several times but not necessarily adsorb (190 μm $>$ depth of channel). The experimental results demonstrate that a significant fraction does not adsorb, which bodes well for the application of this system for the quantitative determination of surface coverage for a particular material set and flow rate, as long-lived adsorption at the outlet window would complicate quantitative analysis.

Representative results for a device that has been pretreated with tetraglyme RF-GDPD and then tested with FITC-BSA show that the trends noted with an untreated device are abolished by the pretreatment step (Fig. 4). All peaks for this experiment superimpose with good precision, as with fluorescein. The representative results for a device that has been pretreated by unlabeled BSA show similar characteristics (ESI†).

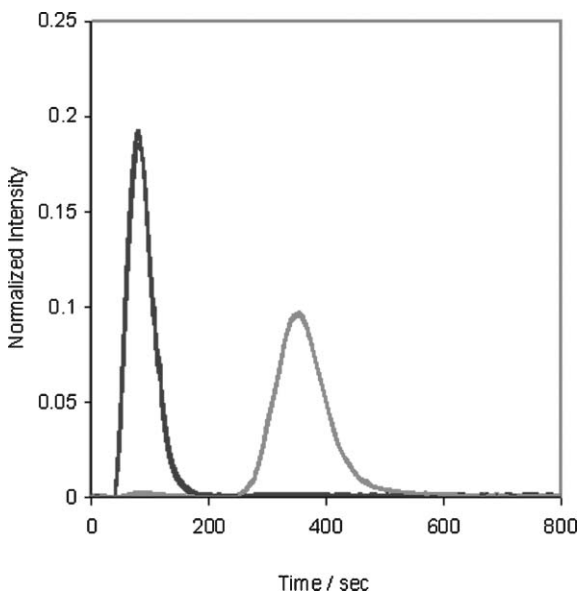

Fig. 4 Five representative runs for FITC-BSA in a device pre-treated by RF-GDPD of tetraglyme. Dark grey lines are observations at the inlet, and light grey lines are observations at the outlet, with the data processing described in the text. A smooth interpolation is used for display. The observed adsorption trend (Fig. 3) is abolished by the pre-treatment.

Quantification of the eluted fraction for each sequential run for these typical experiments also suggests several overall trends (Fig. 5). The negative controls display complete elution of the inlet mass with reasonable precision, $\pm 4\%$ (with the exception of the first three runs of the FITC-dextran experiment) indicating no long-lived adsorption. The positive controls show an upward trend in eluted fraction with sequence number, consistent with a finite number of surface binding sites for the protein.

Since the surface is not cleaned between runs, additional mass introduced in subsequent runs has fewer binding sites available and a greater fraction is eluted. In the lower concentration experiments the eluted fraction never quite reaches unity, indicating the surface is still not saturated. In the higher concentration experiments, the eluted fraction reaches unity after two or three runs, consistent with faster saturation expected from a higher concentration solution. It should be noted that the baseline is reset after each run through the signal processing algorithms, but examination of the raw data (not shown) reveals that there is a constant upward trend in the baseline over the entire experiment. It should also be noted that the normalization algorithm used is probably not appropriate when the inlet window is experiencing a constantly increasing signal due to adsorption, rendering the quantitative values thus obtained slightly suspect. The qualitative trends have been adequately captured, however.

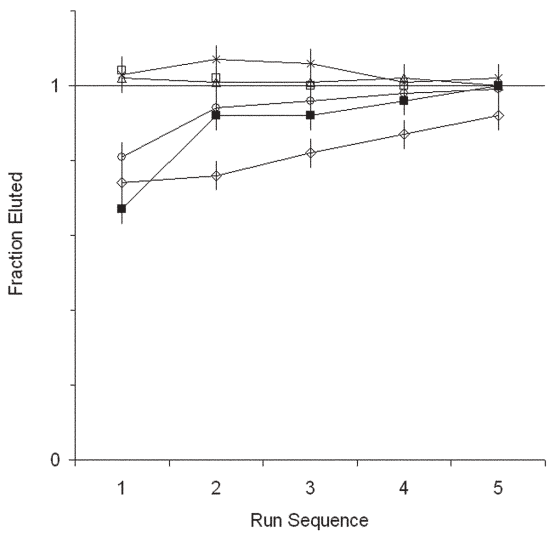

Fig. 5 Fraction of inlet mass eluted, as observed at the outlet, for each of the five sequential runs in the representative experiments shown in Fig. 2–4 and Figs. 1 and 2 of ESI, except 5 M rhodamine, since quantification of those results was invalidated by an experimental artifact (see text). The cardinal numbers correspond to the temporal order in which they were run. The error bars display a standard error derived from replication of the experiments. (△) = 1 M fluorescein, (■) = 2 M FITC-dextran, (◇) = 2 M FITC-BSA, (○) = 20 M FITC-BSA in untreated device, (×) = 20 M FITC-BSA in BSA treated device, (□) = 20 M FITC-BSA in tetragyme/plasma treated device (mostly obscured by 1 M fluorescein results).

It is important when interpreting results from these experiments that the chromatograms of potential adsorbants are compared to negative controls of similar diffusivity. Our results suggest two ways this may be accomplished without resorting to identification of a non-adsorbing species of similar diffusivity (a task whose difficulty is illustrated by the FITC-dextran results). (1) Use of a non-fouling coating will create a negative control; however, that will not be useful if the objective of the experiment is to identify or validate such a coating. (2) A high concentration of the adsorbate may create a negative control if the signal from the unadsorbed fraction is so great that it renders the signal from the adsorbed material undetectable. If the material adsorbs permanently, the device can be pre-treated to saturate the binding sites and to further reduce the signal from adsorption. Thus an adsorbate can be used as its own control. Alternatively, the dispersion of a material of known diffusivity can be calculated with relatively simple analytical expressions, if certain design criteria are met. The device shown (Fig. 1) did not meet those criteria, but a redesigned device did (ESI†), and gave similar performance to the one shown here.

Conclusions

The significance of adsorption of analytes or reagents to realisitic microfluidic devices can be assessed using the approach outlined here. The advantages of the technique demonstrated here include: compatibility with the substrate and basic channel geometry from which the device of interest is made, the ability to detect both transient and long-lived adsorption, and a 'built-in' relevance of results—a positive or negative result is immediately significant with respect to the problem at hand. The disadvantages include: the need for a detectable analyte or labeled version of the analyte (which can change the adsorption behavior relative to an unlabeled version), and the need for an appropriate negative control. Improvements to the data processing algorithms and more accurate modeling of the results will yield a technique that is quantitatively accurate.

Acknowledgements

The authors would like to thank Dr Buddy Ratner and Winston Ciridon at UWEB for performing the tetraglyme coating. This research was supported by NIH grant: 1 R01 RR 15309-01A1

References

1 K. Nakanishi, T. Sakiyama and K. Imamura, *J. Biosci. Bioeng.*, 2001, **91**, 233–244.
2 A. Lionello, J. Josserand, H. Jensen and H. H. Girault, *Lab Chip*, 2005, **5**, 254–260.
3 V. Linder, E. Verpoorte, W. Thormann, N. F. de Rooij and M. Sigrist, *Anal. Chem.*, 2001, **73**, 4181–4189.
4 M. S. Munson, M. S. Hasenbank, E. Fu and P. Yager, *Lab Chip*, 2004, **4**, 438–445.
5 S. Ghosal, *Anal. Chem.*, 2002, **74**, 771–775.
6 C. E. Jordan and R. M. Corn, *Anal. Chem.*, 1997, **69**, 1449–1456.
7 K. C. Popat and T. A. Desai, *Biosens. Bioelectron.*, 2004, **19**, 1037–1044.
8 V. A. Liu, W. E. Jastromb and S. N. Bhatia, *J. Biomed. Mater. Res.*, 2002, **60**, 126–134.
9 Y. Liu, J. C. Fanguy, J. M. Bledsoe and C. S. Henry, *Anal. Chem.*, 2000, **72**, 5939–5944.
10 M. C. Shen, Y. V. Pan, M. S. Wagner, K. D. Hauch, D. G. Castner, B. D. Ratner and T. A. Horbett, *J. Biomater. Sci., Polym. Ed.*, 2001, **12**, 961–978.
11 M. C. Shen, M. S. Wagner, D. G. Castner, B. D. Ratner and T. A. Horbett, *Langmuir*, 2003, **19**, 1692–1699.
12 M. Q. Zhang and M. Ferrari, *Biotechnol. Bioeng.*, 1997, **56**, 618–625.
13 C. G. P. H. Schroen, M. A. C. Stuart, K. V. Maarschalk, A. Vanderpadt and K. Vantriet, *Langmuir*, 1995, **11**, 3068–3074.
14 A. Bange, H. B. Halsall and W. R. Heineman, *Biosens. Bioelectron.*, 2005, **20**, 2488–2503.
15 D. Beyer, W. Knoll, H. Ringsdorf, J. H. Wang, R. B. Timmons and P. Sluka, *J. Biomed. Mater. Res.*, 1997, **36**, 181–189.
16 A. Hatch, E. Garcia and P. Yager, *Proc. IEEE*, 2004, **92**, 126–139.
17 K. R. Hawkins and P. Yager, *Lab Chip*, 2003, **3**, 248–252.